FINGERPRINT RESTORATION USING DIGITAL REACTION-DIFFUSION SYSTEM

Koichi Ito, Takafumi Aoki and Tatsuo Higuchi
Graduate School of Information Sciences, Tohoku University
Aoba-yama 05, Sendai, 980-8579 JAPAN
Phone: +81-22-217-7169, Fax: +81-22-263-9406,
E-mail: ito@higuchi.ecei.tohoku.ac.jp

ABSTRACT

This paper presents an algorithm for fingerprint image restoration using a digital reaction-diffusion system (DRDS). The DRDS is a model of a discrete-time discrete-space nonlinear reaction-diffusion dynamical system, which is useful for generating biological textures, patterns and structures. This paper proposes a special DRDS, called an adaptive DRDS, having the capability of restoring incomplete fingerprint images. The phase-only correlation technique is employed to evaluate the restoration capability of the adaptive DRDS on actual fingerprint images.

1. INTRODUCTION

Living organisms can create a remarkable variety of patterns and forms from genetic information. In embryology, the development of patterns and forms is sometimes called "*Morphogenesis*". In 1952, Alan Turing suggested that a system of chemical substances, called morphogens, reacting together and diffusing through a tissue, is adequate to account for the main phenomena of morphogenesis [1]. From an engineering viewpoint, the insights into morphogenesis provide important concepts for devising a new class of intelligent signal processing algorithm employing biological pattern formation [2].

Inspired by Turing's morphogenesis concept, we have proposed a *Digital Reaction-Diffusion System* (DRDS) – a model of a discrete-time discrete-space reaction-diffusion dynamical system – for understanding the principle of biological pattern formation in the framework of multidimensional digital signal processing [3]. In this paper, we present an application of the DRDS to fingerprint image restoration. The problem considered in this paper is to restore the original fingerprint patterns from blurred fingerprint images. Such consideration will be useful for improving the performance of fingerprint identification systems.

To address this problem, we present a new variation of DRDS, called an adaptive DRDS, which is specially designed for fingerprint restoration tasks. We design the adaptive DRDS to enhance the inherent frequency components in the given fingerprint image adjusting the local orientation of generated patterns adaptively to the given image. In this paper, we propose a restoration algorithm using the adaptive DRDS. The algorithm can reconstruct the original fingerprint patterns even if incomplete fingerprint images are given. The restoration capability of the proposed algorithm is evaluated by using the Phase-Only Correlation (POC) technique, which has already been applied to practical fingerprint identification system by the authors' group [4].

2. DIGITAL REACTION-DIFFUSION SYSTEM

A Digital Reaction-Diffusion System (DRDS) – a model of a discrete-time discrete-space reaction-diffusion dynamical system – can be naturally derived from the original reaction-diffusion system defined in continuous space and time. The general M-morphogen reaction-diffusion system with two-dimensional (2-D) space indices (r_1, r_2) is written as

$$\frac{\partial \tilde{\boldsymbol{x}}(t, r_1, r_2)}{\partial t} = \tilde{\boldsymbol{R}}(\tilde{\boldsymbol{x}}(t, r_1, r_2)) + \tilde{\boldsymbol{D}} \nabla^2 \tilde{\boldsymbol{x}}(t, r_1, r_2), \qquad (1)$$

where

$\tilde{\boldsymbol{x}} = [\tilde{x}_1, \tilde{x}_2, \cdots, \tilde{x}_M]^T$,
$\tilde{x}_i$: concentration of the i-th morphogen,
$\tilde{\boldsymbol{R}}(\tilde{\boldsymbol{x}}) = [\tilde{R}_1(\tilde{\boldsymbol{x}}), \tilde{R}_2(\tilde{\boldsymbol{x}}), \cdots, \tilde{R}_M(\tilde{\boldsymbol{x}})]^T$,
$\tilde{R}_i(\tilde{\boldsymbol{x}})$: reaction kinetics for the i-th morphogen,
$\tilde{\boldsymbol{D}} = diag[\tilde{D}_1, \tilde{D}_2, \cdots, \tilde{D}_M]$,
$diag$: diagonal matrix,
$\tilde{D}_i$: diffusion coefficient of the i-th morphogen.

We now sample a continuous variable $\tilde{\boldsymbol{x}}$ in (1) at the time sampling interval T_0, and at the space sampling intervals T_1 and T_2. Assuming discrete time-index to be given by n_0 and discrete space indices to be given by (n_1, n_2), we have

$$\boldsymbol{x}(n_0, n_1, n_2) = \tilde{\boldsymbol{x}}(n_0 T_0, n_1 T_1, n_2 T_2). \qquad (2)$$

Using this discritization, the general DRDS can be obtained as

$$
\begin{aligned}
&\boldsymbol{x}(n_0+1, n_1, n_2) \\
&\quad = \quad \boldsymbol{x}(n_0, n_1, n_2) + \boldsymbol{R}(\boldsymbol{x}(n_0, n_1, n_2)) \\
&\qquad + \boldsymbol{D}(l * \boldsymbol{x})(n_0, n_1, n_2), \qquad (3)
\end{aligned}
$$

where

$$
\begin{aligned}
\boldsymbol{x} &= [x_1, x_2, \cdots, x_M]^T, \\
\boldsymbol{R} &= T_0 \tilde{\boldsymbol{R}} = [R_1(\boldsymbol{x}), R_2(\boldsymbol{x}), \cdots, R_M(\boldsymbol{x})]^T, \\
\boldsymbol{D} &= T_0 \tilde{\boldsymbol{D}} = diag[D_1, D_2, \cdots, D_M], \\
&l(n_1, n_2) \\
&= \begin{cases} \frac{1}{T_1^2} & (n_1, n_2) = (-1, 0), (1, 0) \\ \frac{1}{T_2^2} & (n_1, n_2) = (0, -1), (0, 1) \\ -2(\frac{1}{T_1^2} + \frac{1}{T_2^2}) & (n_1, n_2) = (0, 0) \\ 0 & \text{otherwise,} \end{cases}
\end{aligned}
$$

and $*$ is the spatial convolution operator defined as

$$
\begin{aligned}
&(l * \boldsymbol{x})(n_0, n_1, n_2) \\
&= \begin{bmatrix} (l * x_1)(n_0, n_1, n_2) \\ (l * x_2)(n_0, n_1, n_2) \\ \vdots \\ (l * x_M)(n_0, n_1, n_2) \end{bmatrix} \\
&= \begin{bmatrix} \sum_{p_1=-1}^{1} \sum_{p_2=-1}^{1} l(p_1, p_2) x_1(n_0, n_1 - p_1, n_2 - p_2) \\ \sum_{p_1=-1}^{1} \sum_{p_2=-1}^{1} l(p_1, p_2) x_2(n_0, n_1 - p_1, n_2 - p_2) \\ \vdots \\ \sum_{p_1=-1}^{1} \sum_{p_2=-1}^{1} l(p_1, p_2) x_M(n_0, n_1 - p_1, n_2 - p_2) \end{bmatrix}.
\end{aligned}
$$

The DRDS described by (3) can be understood as a 3-D nonlinear digital filter. We first store an initial (input) image in a specific morphogen, say $x_i(0, n_1, n_2)$, at time 0. After computing the dynamics for n_0 steps, we can obtain the output image from one of the M morphogens, say $x_i(n_0, n_1, n_2)$, at time n_0. In general, linear digital filters with guaranteed stability are widely used in many signal processing applications. In our application, however, we employ the DRDS with nonlinear reaction kinetics $\boldsymbol{R}(\boldsymbol{x})$ satisfying the diffusion-driven instability condition [3]. In this case, DRDS becomes an unstable 3-D nonlinear digital filter having significant pattern formation capability.

In this paper, we use the two-morphogen DRDS ($M = 2$) with the Brusselator reaction kinetics, which is one of the most widely studied chemical oscillators [5]. The two-morphogen Brusselator-based DRDS is defined as follows:

$$
\begin{aligned}
\begin{bmatrix} x_1(n_0+1, n_1, n_2) \\ x_2(n_0+1, n_1, n_2) \end{bmatrix} &= \begin{bmatrix} x_1(n_0, n_1, n_2) \\ x_2(n_0, n_1, n_2) \end{bmatrix} \\
&+ \begin{bmatrix} R_1(x_1(n_0, n_1, n_2), x_2(n_0, n_1, n_2)) \\ R_2(x_1(n_0, n_1, n_2), x_2(n_0, n_1, n_2)) \end{bmatrix} \\
&+ \begin{bmatrix} D_1(l * x_1)(n_0, n_1, n_2) \\ D_2(l * x_2)(n_0, n_1, n_2) \end{bmatrix}, \qquad (4)
\end{aligned}
$$

where

$$
\begin{aligned}
R_1(x_1, x_2) &= k_1 - (k_2 + 1)x_1 + x_1^2 x_2, \\
R_2(x_1, x_2) &= k_2 x_1 - x_1^2 x_2.
\end{aligned}
$$

In this paper, we employ the parameter set: $k_1 = 2$, $k_2 = 4$, $T_0 = 0.01$, $D_1 = 0.01$ and $D_2 = 0.05$.

3. ADAPTIVE DRDS FOR FINGERPRINT RESTORATION

This section proposes a restoration algorithm for blurred fingerprint images using an adaptive DRDS. We also discuss the experimental results of fingerprint image restoration using the proposed algorithm.

3.1 Restoration Algorithm for Blurred Fingerprint Images

The DRDS with spatially isotropic diffusion terms has produced some broken ridge lines in processing fingerprint images, since it does not take account of the local orientation of ridge flow. In order to solve this problem, we present an adaptive DRDS model, in which we can use the local orientation of the ridge flow in a fingerprint image to guide the action of DRDS. This can be realized by introducing orientation masks to be convolved with the diffusion terms in DRDS (3).

In this paper, we define a two-morphogen adaptive DRDS with the Brusselator reaction kinetics. The two-morphogen adaptive DRDS can be written as

$$
\begin{aligned}
\begin{bmatrix} x_1(n_0+1, n_1, n_2) \\ x_2(n_0+1, n_1, n_2) \end{bmatrix} &= \begin{bmatrix} x_1(n_0, n_1, n_2) \\ x_2(n_0, n_1, n_2) \end{bmatrix} \\
&+ \begin{bmatrix} R_1(x_1(n_0, n_1, n_2), x_2(n_0, n_1, n_2)) \\ R_2(x_1(n_0, n_1, n_2), x_2(n_0, n_1, n_2)) \end{bmatrix} \\
&+ \begin{bmatrix} D_1(h_1^{n_1 n_2} * l * x_1)(n_0, n_1, n_2) \\ D_2(h_2^{n_1 n_2} * l * x_2)(n_0, n_1, n_2) \end{bmatrix}, \qquad (5)
\end{aligned}
$$

where

$h_i^{m_1 m_2}(n_1, n_2)$: orientation mask at the pixel (m_1, m_2) for the i-th morphogen,

$R_1(x_1, x_2)$, $R_2(x_1, x_2)$: the Brusselator reaction kinetics.

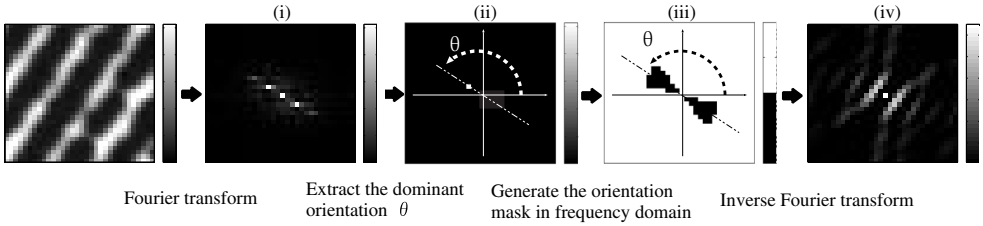

Fig. 1: Generation of the orientation mask.

In the above equation, we define the orientation mask $h_1^{m_1 m_2}(n_1, n_2)$ at the pixel (m_1, m_2) as a 32×32 matrix having real coefficient values within the window $(n_1, n_2) = (-16, -16) \sim (15, 15)$, which can be automatically derived as follows (Fig. 1): (i) take the Fourier transform of the local image around the pixel (m_1, m_2), (ii) extract the dominant ridge orientation θ from the transformed image, (iii) generate a mask pattern $H_1^{m_1 m_2}(j\omega_1, j\omega_2)$ having the orientation θ in frequency domain as

$$H_1^{m_1 m_2}(j\omega_1, j\omega_2) = \begin{cases} 1 & \text{for unstable frequency band} \\ & \text{(black pixels in Fig. 1(iii))} \\ 2 & \text{otherwise,} \end{cases}$$

and (iv) take the inverse Fourier transform to obtain the orientation mask $h_1^{m_1 m_2}(n_1, n_2)$. The orientation mask $h_2^{m_1 m_2}(n_1, n_2)$ for the second morphogen, on the other hand, has the value 1 at the center $(n_1, n_2) = (0, 0)$, and equals to 0 for other coordinates (n_1, n_2). Thus, the dynamics for the morphogen $x_2(n_0, n_1, n_2)$ does not take account of the local orientation.

In this paper, we consider the problem of restoring the original fingerprint images from blurred fingerprint images. In order to process fingerprint images, spatial sampling parameters T_1 and T_2 should be adjusted according to the inherent spatial frequency of fingerprint images. Let assume that a set of exact orientation masks $\boldsymbol{h}^{m_1 m_2}(n_1, n_2)$ has already been obtained. We first set the initial (blurred) fingerprint image in $x_1(0, n_1, n_2)$, at time 0. The dynamics given by (5) has the equilibrium $(x_1, x_2) = (2, 2)$, and the variation ranges of variables (x_1, x_2) are bounded around the equilibrium point as $1 \leq x_1 \leq 3$ and $1 \leq x_2 \leq 3$ in the case of given parameter set. Hence, we first scale the [0,255] gray-scale fingerprint image into [1,3] range. The scaled image becomes the initial input $x_1(0, n_1, n_2)$, while the initial condition of the second morphogen is given by $x_2(0, n_1, n_2) = 2$ (equilibrium). The zero-flux Neumann boundary condition is employed for computing the dynamics. After n_0 steps of the

procedure *Adaptive DRDS with Hierarchical Orientation Estimation*

```
1.  begin
2.    p := 2;
3.    while time step n_0 equals to 500 do
4.    begin
5.      if image partitioning factor p is less than 9 then
6.      begin
7.        partition the input image into p^2 sub-images;
8.        generate independent orientation masks
          for p^2 sub-images;
9.        run the adaptive DRDS (Eq.(5))
          for 10 time steps;
10.       p := p + 1
11.     end
12.     else
13.     begin
14.       generate independent orientation masks
          for all pixels;
15.       run the adaptive DRDS (Eq.(5))
          for 10 time steps
16.     end
17.   end
18. end.
```

Fig. 2: Algorithm for the adaptive DRDS with hierarchical orientation estimation.

adaptive DRDS computation, we obtain $x_1(n_0, n_1, n_2)$ as the output image, which is scaled back into the [0,255] gray-scale image to produce the final output.

In practical situation, it is difficult to obtain the exact orientation masks from blurred fingerprints. Addressing this problem, we propose a method of estimating local orientation masks recursively using a coarse-to-fine approach as shown in Fig. 2. This restoration algorithm starts with rough estimation of local orientation for 2×2 sub-images. The image partitioning factor p gradually

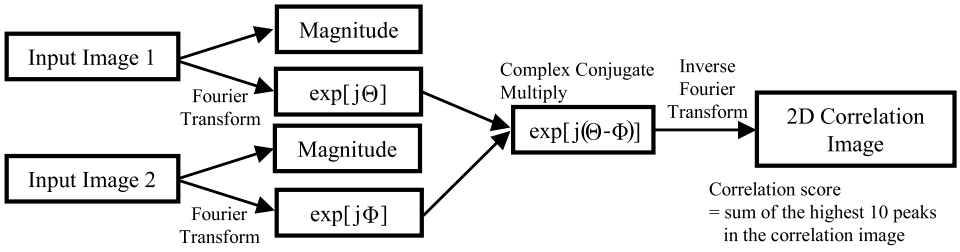

Fig. 3: Computation flow of Phase-Only Correlation (POC).

increases as restoration step n_0 increases. We can obtain pixel-wise orientation masks $\boldsymbol{h}^{m_1 m_2}(n_1, n_2)$ after 80 time steps. This makes possible significant improvement in the precision of orientation estimation.

3.2 Experiment

This subsection shows an experiment for evaluating restoration performance of the proposed algorithm. We consider the problem of restoring the original fingerprint image from its "subsampled" image. For this purpose, we generate a subsampled fingerprint image from the original fingerprint image as follows: (i) partition the original image into $R \times S$-pixel rectangular blocks, and (ii) select one pixel randomly from every block and eliminate all the other pixels (set 127 to the pixels). The image thus obtained has the same size as the original image, but the number of effective pixels is reduced to $1/(R \times S)$.

The restoration capability of the proposed algorithm is evaluated by calculating the similarity between the original fingerprint image and the restored image. To measure the similarity, we employ the Phase-Only Correlation (POC) [4], which has an efficient discrimination capability in fingerprint identification tasks. Figure 3 shows the computation flow of POC. In this experiment, we use ten distinct fingerprints (Sample01–Sample10). Restoration experiments are carried out for various subsampling rates $1/(3\times3)$, $1/(3\times4)$, $1/(4\times4)$, $1/(4\times5)$, $1/(5\times5)$, $1/(5\times6)$, $1/(6\times6)$, $1/(6\times7)$, $1/(7\times7)$, $1/(7\times8)$ and $1/(8\times8)$.

3.3 Result and Discussion

This subsection focuses on the result of restoring the $1/(5\times5)$ subsampled image. Figure 4 (a) shows the original image, the subsampled image ($n_0 = 0$) and restored images at $n_0 = 100$, 200 and 400, respectively. Figure 4 (b) shows the angle for each pixel. We can observe that the proposed algorithm estimates the exact orientation from a subsampled fingerprint image as time step increases.

We discuss the evaluation of the above restoration result in the followings. Figure 5 shows the variation of correlation scores calculated between the original image of Sample04 and the restored images of Sample01–Sample10 for the case of subsampling rate $1/(5\times5)$. We can confirm that the similarity between the original Sample04 and the corresponding restored image increases as the number of steps n_0 increases. The optimal discrimination capability could be obtained at around $n_0 = 400$ steps, which is indicated with a vertical dashed line in this figure. The horizontal dashed line indicates the threshold for discrimination. In the range of n_0 =100–300 steps, the correlation scores for the incorrect fingerprints drop steeply while the correct fingerprint keeps sufficient level of correlation.

Table 1 shows the success rate of fingerprint identification for various subsampling rates. In the case where the subsampling rates are from $1/(3\times3)$ to $1/(5\times5)$, we can restore the subsampled images completely. This experiment demonstrates a potential capability of adaptive DRDS to enhance the performance of matching algorithms for blurred fingerprint images. On the other hand, it becomes difficult to generate the exact orientation masks as the subsampling rate increases. Further improvement of restoration performance may be possible by using a deformable fingerprint model for adjusting orientation masks, which remains as a future work.

4. CONCLUSION

This paper presents an application of the DRDS to restoration of fingerprint images. Using the adaptive DRDS, we design the restoration algorithm which has the capability to reconstruct a complete fingerprint pattern from a blurred image and evaluate its restoration performance. From experimental results, the proposed algorithm has the effective restoration capability to identify blurred fingerprint images.

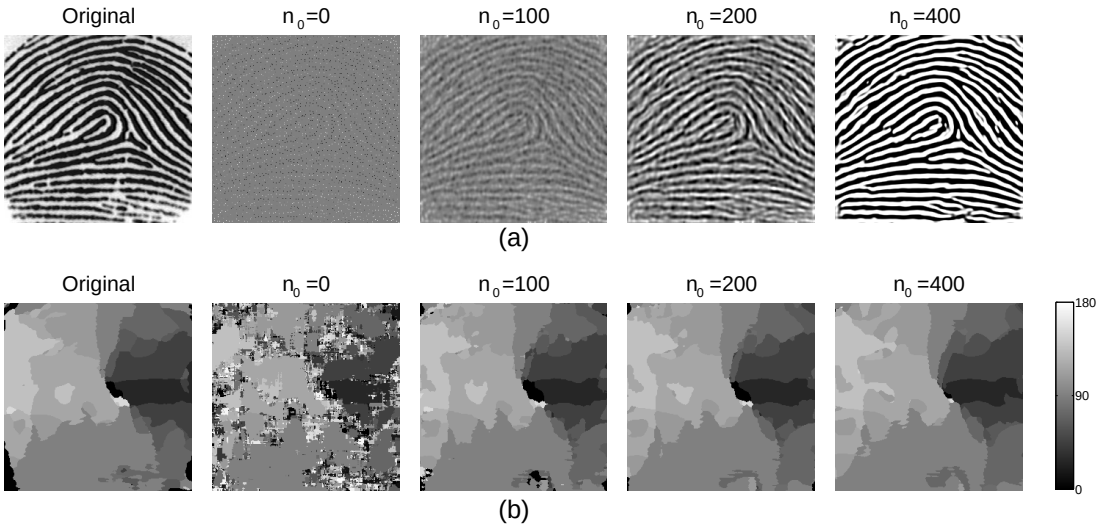

Fig. 4: Fingerprint restoration from a subsampled image (*Sample04*) with subsampling rate $1/(5 \times 5)$: (a) the original image, subsampled image ($n_0 = 0$) and restored images, (b) the corresponding visualized angle.

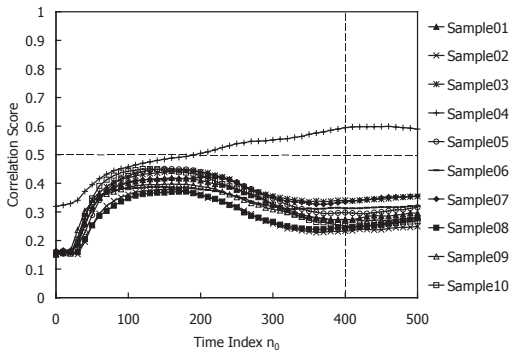

Fig. 5: Correlation scores between the original image of *Sample04* and the restored images of Sample01–Sample10 (restoration from $1/(5 \times 5)$ subsampled images).

Table 1: Identification rate.

Subsampling Rate	Number of Identified Samples	Identification Rate
$1/(3 \times 3)$	10	100%
$1/(3 \times 4)$	10	100%
$1/(4 \times 4)$	10	100%
$1/(4 \times 5)$	10	100%
$1/(5 \times 5)$	10	100%
$1/(5 \times 6)$	9	90%
$1/(6 \times 6)$	6	60%
$1/(6 \times 7)$	3	30%
$1/(7 \times 7)$	3	30%
$1/(7 \times 8)$	1	10%
$1/(8 \times 8)$	0	0%

REFERENCES

[1] A. M. Turing, "The chemical basis of morphogenesis," Phil. Trans. R. Soc. London, Vol.B237, pp.37–72, Aug. 1952.

[2] A. S. Sherstinsky and R. W. Picard,"M-Lattice: From morphogenesis to image processing," IEEE Trans. Image Processing, vol.5, no.7, pp.1137-1150, July 1996.

[3] K. Ito, T. Aoki, and T. Higuchi, "Digital reaction-diffusion system — A foundation of bio-inspired texture image processing —," IEICE Trans. Fundamentals, Vol.E84-A, No.8, pp.1909–1918, Aug. 2001.

[4] K. Kobayashi, "Phase-only correlation chips and its vision sensing applications,"(in Japanese), Journal of the society of instrument and control engineers, Vol.40, No.12, pp.902–906, Dec. 2001.

[5] J. D. Murray, "Mathematical Biology," Springer-Verlag, Berlin, 1993.